50 shades of colour: how thickness, iron redox and manganese/antimony contents influence perceived and intrinsic colour in Roman glass

Anne-Isabelle Bidegaray[1,2,3], Karin Nys[3], Alberta Silvestri[4*], Peter Cosyns[3], Wendy Meulebroeck[5], Herman Terryn[1], Stéphane Godet[2], Andrea Ceglia[5]

[1] Department of Electrochemical and Surface Engineering, SURF Research Group, Vrije Universiteit Brussel, Pleinlaan 2, 1050 Brussels, Belgium

[2] Materials Engineering, Characterization, Processing and Recycling, 4MAT, Université libre de Bruxelles, 50 Avenue Franklin Roosevelt, CP165/63, 1050 Brussels, Belgium

[3] Department of Art Sciences and Archaeology, MARI Research Group, Vrije Universiteit Brussel, Pleinlaan 2, 1050 Brussels, Belgium

[4] Department of Geosciences, University of Padova, via Giovanni Gradenigo 6, 35131 Padova, Italy

[5] Department of Applied Physics and Photonics, Brussels Photonics Team B-PHOT, Vrije Universiteit Brussel, Pleinlaan 2, 1050 Brussels, Belgium

Abstract

Roman glass is studied here by means of optical absorption spectroscopy, in order to provide an objective method to quantitatively evaluate colour. The dataset is composed of 165 soda-lime-silicate glass samples from various western European sites, mainly dated from the 1st to 4th century AD, and containing variable amounts of iron, manganese and/or antimony. Iron redox ratios and colour coordinates (based on the CIELab colour system) are determined and put in relation with the thickness of samples and their manganese/antimony contents. Results reveal thickness as a crucial parameter when discussing glass hues, thus leading to a differentiation between the 'intrinsic' and perceived' colour of glass objects (i.e., the colour of the object with the thickness normalised to 1 mm, and that with its original thickness, respectively). Apart from HIMT and purple glass, the concentration of ferrous iron appears to be correlated with a*— a colourimetric parameter determining how green the glass is. Significant relations of antimony/manganese contents versus iron redox and glass colour are also considered, resulting in quantitative arguments to entitle antimony-decoloured glass as the most oxidised and colourless glass.

Key words: Roman glass, optical absorption spectroscopy, colour, antimony, manganese, iron redox

* Corresponding author. E-mail: alberta.silvestri@unipd.it; telephone: 0039-049-8279142; ORCID iD: 0000-0001-9747-3194.

1. Introduction

Colour is one of the most intriguing features of glass and it is produced by a complex combination of chemical and structural effects. It is mainly due to the presence of transition metal ions (e.g., Fe^{2+}/Fe^{3+}, Co^{2+}, Cu^{2+}, Mn^{3+}), which cause selective absorption of electromagnetic radiation in the visible band and act as colouring agents or chromophores (Weyl 1951; Bamford 1977; Calas et al. 2002; Möncke et al. 2014). Other colouring effects can be produced when a metal is dispersed as minute particles in the glass, the colour depends on the size of the colloidal dispersion (Newton and Davison 1996). Lastly, colour may also be due to pigments dispersed in the matrix (e.g., lead antimonate or cuprite), which not only colour glass but also opacify it, due to diffusion of incident radiation, generated by refraction between the glassy matrix and microcrystalline areas within the glass itself (Biron and Chopinet 2013).

The present paper focuses on colour variations due to iron, which is an almost ubiquitous multivalent element generally present in ancient glass as an impurity from various minerals in sand (Aerts et al. 2003), and on the impact of manganese and antimony in neutralizing the colouring effects of iron presence. Both iron concentration and the iron redox state have a key influence on glass colour. While high concentrations of iron oxide cause the glass to appear black (above 5 wt% of Fe_2O_3, glass will appear black; Van Der Linden et al. 2009; Cosyns 2011; Cagno et al. 2013, 2014; Ceglia et al. 2014), the redox state of iron affects glass hues in a more subtle way. The presence of reduced iron (ferrous) causes a blue-green colour, whereas oxidised iron (ferric) generates a yellowish tinge (Newton and Davison 1996). To get rid of the above undesirable hues, ancient glassmakers added manganese and/or antimony oxides (Sayre 1963; Jackson 2005; Gliozzo et al. 2016). Glass science and archaeometric literature generally consider that both antimony and manganese oxidise iron from its reduced blue-green state to its oxidised yellowish state (e.g., (Bamford 1977; Schreiber 1987; Newton and Davison 1996; Janssens 2013)). Previous studies on the chronological trend of manganese and antimony use suggest that antimony was rather preferred in the earlier stages of the Roman imperial period and gradually lost prominence in favour of manganese (Paynter and Jackson 2016; Gliozzo 2017). Although manganese or antimony oxides would have been sufficient individually to decolour glass by oxidising the iron, ancient glass, containing both oxides, is encountered frequently in many archaeological sites all over the Roman Empire. This has been generally attributed to glass recycling, whereby manganese and antimony decoloured glass fragments were mixed and remelted together e.g., (Silvestri 2008; Foster and Jackson 2010; Freestone 2015; Jackson and Paynter 2015; Maltoni et al. 2016; Silvestri et al. 2018). Aside from these three compositional groups of colourless glass (Sb-colourless or Roman antimony decoloured glass, Mn-colourless or Roman manganese decoloured glass, Mn/Sb-colourless or Roman mixed antimony and manganese glass e.g., (Jackson 2005; Paynter 2006; Jackson and Paynter 2015; Gliozzo 2017; Schibille et al. 2017; Silvestri et al. 2018)), a fourth one is characterised

by the absence of both decolouring agents, and its colourless appearance is due to very little amounts of iron. Although this type of glass is not frequently demonstrated (Gliozzo 2017), its production implies that ancient glassmakers had knowledge to carefully select raw materials with low levels of impurities. In addition, specific composition of Late Antique glass containing iron, as the only chromophore, and manganese, as the only decolouriser, both in high amounts (Fe_2O_3 and MnO > 1 wt%), is classified as High Iron Manganese Titanium (HIMT) glass (Freestone 1994; Freestone et al. 2018).

How manganese and antimony interact with iron is a complex problem. First, ancient glasses with similar chemical compositions in terms of iron, manganese and antimony can have different colours. It was found that Roman manganese-decoloured glass contains 1.10 ± 0.63 wt% MnO on average (Gliozzo 2017), while the manganese oxide concentration in purple glass can go from 0.95 to 3.82 wt% (Mirti et al. 2008; Van Der Linden et al. 2009; Arletti et al. 2010; Ganio et al. 2012; Gallo et al. 2013; Arletti et al. 2013; Cagno et al. 2014; Cosyns et al. 2014; Silvestri et al. 2014; Möncke et al. 2014; Rosenow and Rehren 2014; Freestone and Stapleton 2015; Rehren et al. 2015; Bonnerot et al. 2016; Schibille et al. 2016; Boschetti et al. 2017). Just to give an example, a purple toilet glass from Adria was found with 1.55 wt% MnO and 0.37 wt% Fe_2O_3 (Gallo et al. 2013) and a greenish glass flask from Aquileia contained 1.93 wt% MnO and 0.54 wt% Fe_2O_3 (Maltoni et al. 2016). There are, thus, glasses with very similar amounts of iron and manganese that appear either purple, colourless, or green. Second, archaeometry on the one hand and chemistry or materials science on the other provide contradictory interpretations of the interaction of multivalent elements: while manganese is considered more effective at oxidising iron than antimony in modern glass science (Schreiber et al. 1984, 2000; Donald et al. 2006), previous study on chromophores in archaeological glass has suggested the opposite (Arletti et al., 2013). As remarked by Gliozzo (2017) and Ceglia et al. (2016), the labelling of glass as colourless or naturally coloured, made by the naked eye, is also particularly ambiguous and depends both on physical extrinsic parameters, such as the type of light, and intrinsic ones of sample, such as its thickness and preservation condition. In addition, the interpretation of the glass hue by the naked eye is subjective, so that colour description of ancient glass is highly operator dependent (Johnston-Feller 2001). In such context, it should be stressed that determination of the oxidation state of transition metal ions in ancient glass, to determine causes of colour, is a long standing question and previous studies on this topic were carried out mainly by means of X-ray absorption spectroscopy and/or other techniques, such as optical absorption spectroscopy and electron paramagnetic resonance, and were focused on a large variety of ancient glasses not only dated to Roman times but also to the Middle Ages (e.g., (Azzoni et al. 2005; Quartieri et al. 2005; Bingham and Jackson 2008; Meulebroeck et al. 2010; Gliozzo et al. 2010; De Ferri et al. 2011; Arletti et al. 2013; Ceglia et al. 2014,

2016; Möncke et al. 2014; Zoleo et al. 2015; Hunault et al. 2016, 2017; Capobianco et al. 2019). It should also be highlighted that, with optical and X-ray spectroscopies, the determination of the redox ratio of iron is easier than for other metals such as manganese (Bamford 1977; Bidegaray et al. 2018). Notwithstanding such studies based on different analytical tools, important archaeological questions about ancient glass colouring technology are still awaiting answers: for instance, how Roman glassworkers coloured or decoloured glass?

The aim of this paper is, therefore, to address Roman glass colouring and decolouring technologies, by considering the correlated impact of iron redox, antimony/manganese contents, and thickness on the glass colour. Thus, we systematically analyse the links among these four important aspects and discuss the extent to which they could have influenced each other. This makes a comparison between manganese and antimony glass, as well as an assessment of the possible optical properties. To address these issues, an ample dataset of Roman glass from various western European sites is analysed using optical absorption spectroscopy.

2. Materials and methods

2.1. Materials

The dataset was composed of 165 soda-lime silica glass objects, mainly dated from the 1st to 4th century AD and coming from various European sites in the Mediterranean (Iulia Felix, Ouest Embiez 1, Adria, Padova, and San Genesio) and Oudenburg in Belgium. The total sample set encompassed 205 measurements, because some fragments with variable thicknesses within the single piece were measured on multiple spots and treated as different samples. These supplementary data were made identifiable by adding a letter (b or c) to the end of sample label (Appendix). The present dataset was previously characterised by the chemical point of view and results are detailed elsewhere (Silvestri et al. 2008, 2014; Silvestri 2008; Ganio et al. 2012; Gallo et al. 2013; Mendera et al. 2017; Bidegaray et al. 2019); here it is analysed using optical absorption spectroscopy.

All analysed samples were natron-based glasses, with variable amounts of iron, manganese, and/or antimony and no other chromophores. In general, the majority of samples could be classified as colourless or naturally coloured, and they were selected in order to collect the main compositional glass groups of the Roman imperial period (i.e., Sb-colourless, Mn-colourless, Mn/Sb-colourless and naturally coloured glass (e.g., (Jackson 2005; Paynter 2006; Jackson and Paynter 2015; Gliozzo 2017; Schibille et al. 2017; Silvestri et al. 2018)), which are here grouped together based on the presence or

absence of decolouring agents (antimony and manganese) and, therefore, re-named as Sb-glass, Mn-glass and Mn-Sb glass. However, the sample set also contained a few HIMT and purple samples and a single sample with iron, but no manganese and antimony, which is defined as "Fealone". These were also taken into consideration for an advanced verification of potential interrelations between iron redox, manganese contents, and glass colour, in samples characterised by high contents of iron and manganese (HIMT), by manganese as main colourant (purple glass), and by iron as the only colourant, and no decolourants (Fe-alone).

Finally, we synthesised one sample without any colouring or decolouring elements, and it was used here as a reference for colourless glass.

2.1.1 Iulia Felix

Ninety-four of the glass fragments came from the *Iulia Felix* shipwreck, dated using ceramic seriation to the 3rd century AD. This ship of the 'corbita' type was found approximately 10 km off the coast of Grado, in the northern part of the Adriatic Sea (DMS coordinates: 45° 38' 0.096" N, 13° 16' 23.131" E)[†]. The cargo contained a barrel filled with more than 11,000 fragments of glass weighing 140 kg and traded in view of remelting and recycling (Toniolo 2007). The fragments were identified as cups, bottles, and plates and were organised, according to hierarchical cluster analysis of their chemical compositions, into three groups of colourless glass, Cl1 , Cl2, and Cl1/2 (Silvestri et al. 2008), and four groups of naturally coloured glass, Ic1a, Ic1b, Ic2a, and Ic2b (Silvestri 2008).

Amongst the glass classified as colourless by Silvestri et al. (2008), we analysed 28 fragments from group Cl1 containing antimony as the only decolouring agent, nine samples from group Cl2 containing only manganese as decolourant, and seven samples from group Cl1/2 containing both manganese and antimony. There were thus 44 colourless samples analysed. Amongst the 50 glass fragments classified as naturally coloured by Silvestri (2008), 11 samples from Ic1a, 15 from Ic2a, 21 from Ic1b, and three from Ic2b were analysed. In groups Ic1a, Ic2a and Ic2b, manganese was the only decolouring agent, whereas group Ic1b contains both manganese and antimony. This latter group has been estimated to be based on the recycling of 54% of antimony decoloured glass (Silvestri 2008).

[†] DMS coordinates refer to approximate location of shipwreck and were collected by means of Google Maps.

2.1.2 Embiez

The shipwreck Ouest Embiez 1 sank not far from the Hyeres Isles on the Mediterranean coast of France (DMS coordinates: 43° 4' 49.174" N, 5° 45' 24.502" E)[‡] between the end of the 2nd century and the beginning of the 3rd century AD. At present, it is the only known Roman ship fully dedicated to the trade of glass, containing not only 15 to 18 tonnes of raw glass, but also different types of windowpanes and a large set of cups piled up in wooden cases (Fontaine and Foy 2007). A selection of 18 colourless samples from the Ouest Embiez 1 shipwreck, representing the three types identified (raw glass, windowpanes, and cups), were previously analysed for elemental compositions and results showed the presence of both antimony and manganese decoloured glass (Ganio et al., 2012). Two samples containing antimony as decolourant (Ganio et al. 2012) were included in the present study.

2.1.3 Adria

Adria in Italy was one of the most important ports of the northern part of the Adriatic Sea (DMS coordinates: 45° 2' 58.063" N, 12° 3' 19.703" E)[§] from the 6th century BC until the 2nd century AD (Fogolari and Scarfì 1970). A selection of 61 intentionally coloured or decoloured Roman glass samples of the 1st through 2nd centuries AD coming from Adria and now housed into Archaeological Museum of the town (Bonomi 1996) were texturally (SEM-EDS), mineralogically (XRPD), and chemically (XRF, EPMA, LA-ICP-MS) characterised (Gallo et al. 2013). Although no relationships were identified among chemical compositions (most are close to the typical natron-based Roman glass), vessel types, or production techniques of Adria glass, a dependence on bulk composition was identified for some particular colours, revealing the careful and intentional selection of raw materials. This is, for instance, the case of Sb-colourless glass (group AD/N2) produced with pure sand with low levels of impurities (Gallo et al. 2013). Therefore, three Adria samples of compositional group AD/N2 and dated to the 2nd century AD (Gallo et al. 2013) were added to the sample set.

2.1.4 Oudenburg

Oudenburg is a Roman fortress in Belgium, 8 km inland from the North Sea (DMS coordinates: 51° 11' 5.273" N, 3° 0' 11.761" E)[**]. The *castellum* has four distinguishable layers and is preceded by a pre-fortress level that includes a civil settlement (*vicus*), allowing the site to be dated between the 1st century AD and the beginning of the 5th century AD, though the fortress only started at the end of the

[‡] DMS coordinates refer to approximate location of shipwreck and were collected by means of Google Maps.
[§] DMS coordinates refer to location of Archaeological Museum of Adria and were collected by means of Google Maps.
[**] DMS coordinates refer to location of Oudenburg City Hall and were collected by means of Google Maps.

196 2nd century AD and does not show permanent use (Vanhoutte 2007). It nevertheless represents a
197 relatively long-lived site in the northwestern provinces along important cross-channel trade routes
198 between the Rhine region and Britain. An earlier chemical study on a selection of 90 colourless and
199 naturally coloured glasses, covering the different archaeological sequences, identified various
200 compositional groups: antimony-only, manganese-only, mixed antimony-manganese, HIMT, and one
201 glass without any decolouring agent (Bidegaray et al. 2019). Included in the present study were seven
202 antimony samples, five manganese samples, 36 mixed manganese-antimony samples, 11 HIMT
203 samples, and one "Fe alone" sample (i.e., glass with iron as the only colouring element and no
204 decolouring agents).
205

206 *2.1.5 Purple glass*
207 Six purple glass samples, chemically characterised in previous studies (Gallo et al. 2013; Silvestri et al.
208 2014; Mendera et al. 2017), were added to the present dataset. In particular, three fragments from
209 Adria (DMS coordinates: 45° 2' 58.063" N, 12° 3' 19.703" E)[††] were from blown vessels that were dated
210 to the 1st century AD (Gallo et al. 2013). Additionally, another three samples were analysed: one
211 fragment of a globular purple beaker with *lattimo* thread, probably dated to the 9th century AD coming
212 from the Medieval site of San Genesio (DMS coordinates: 43° 41' 30.574" N, 10° 52' 58.577" E)[‡‡] located
213 in Italy at the junction of important roads (the pilgrims road *via Francigena* and the road between
214 Florence and Pisa) and rivers (*Arno* and *Elsa*) (Mendera et al. 2017) and two purple tesserae from the
215 disrupted paleo-Christian glass mosaic of San Prosdocimus in Padova (NE Italy; DMS coordinates: 45°
216 23' 47.411" N, 11° 52' 47.510" E)[§§] dated to the 6th century AD (Silvestri et al. 2014).

217 Although the glass samples from Padova and San Genesio are dated beyond the main chronological
218 range considered here, their chemical compositions (Silvestri et al. 2014; Mendera et al. 2017) are
219 perfectly comparable with purple glass from the Roman imperial period (Van Der Linden et al. 2009;
220 Gallo et al. 2013; Cagno et al. 2014); therefore, they were selected and analysed in the present study.
221

[††] DMS coordinates refer to location of Archaeological Museum of Adria and were collected by means of Google Maps.
[‡‡] DMS coordinates refer to approximate location of archaeological site and were collected by means of Google Maps.
[§§] DMS coordinates refer to Basilica of St. Justine, inside which the chapel of St. Prosdocimus is located, and were collected by means of Google Maps.

2.1.6 Reference colourless glass

One glass sample, having chemical composition comparable to Roman glass but without iron (70.2 wt% SiO_2, 17.0 wt% Na_2O, 8.8 wt% CaO, 2.48 wt% Al_2O_3, 0.64 wt% K_2O, 0.57 wt% MgO, and 0.19 wt% SO_3), was reproduced in a modern electrical furnace. The sample was synthesised using a 100 g mixture of SiO_2, Na_2CO_3, $CaCO_3$, Al_2O_3, MgO, K_2CO_3 and Na_2SO_4, with a minimum purity of 99.1% of the added chemicals. The raw materials were melted 32 h at 1200°C in a Pt-Rh crucible of 6 cm diameter in an electrical furnace and annealed 12 h at 500°C. The chemical composition was verified by means of Wavelength Dispersive X-ray Fluorescence (WD-XRF, Siemens Bruker S4 PIONEER, Cu Kα radiation, standardless mode). This glass was used as a reference for a colourless glass containing no colouring or decolouring agents.

The averages and standard deviations of main elements of the present dataset are given in Table 1. It should be stressed that, although chemical data of the glass considered here, except for reference glass, were determined in previous studies by means of different analytical methods and instruments during a span of about 10 years (Silvestri et al. 2008, 2014; Silvestri 2008; Ganio et al. 2012; Gallo et al. 2013; Mendera et al. 2017; Bidegaray et al. 2019), the results are perfectly comparable on the basis of the good precision and accuracy of the different techniques for major and minor elemental analysis. Precision and accuracy of all the measurements were, in fact, checked by the repeated analyses of international standards Corning glass A, B, C, and/or D, and they are both 10% better for all major and minor elements reported in Table 1. For instance, considering the worst-case scenario with 10% precision and accuracy, a 0.3 wt% Fe_2O_3 concentration will result in a range of 0.27–0.33 wt%. Therefore, for all elements discussed here (i.e., iron, manganese and antimony), the between-group variation, meaning the difference between group averages, was higher than the analytical variability, as also demonstrated by relative standard variations of iron, manganese and antimony calculated among the considered groups, which are higher than 10%.

***Table 1**. Average (μ) chemical composition (in wt%) and standard deviation (σ) of compositional groups from the Iulia Felix, les Embiez, Oudenburg, Adria, of purple glass set, and the reference colourless glass; n: number of samples of each group; n.a.: not added. Raw data of Iulia Felix glass from (Silvestri et al. 2008; Silvestri 2008); of Embiez from (Ganio et al. 2012); of Adria and purple glass from (Gallo et al. 2013; Silvestri et al. 2014; Mendera et al. 2017), of Oudenburg from (Bidegaray et al. 2019).*

	group		n	SiO_2	Na_2O	CaO	Al_2O_3	K_2O	MgO	Fe_2O_3	TiO_2	MnO	Sb_2O_3	P_2O_5
Embiez	Sb	μ	2	70.1	19.46	5.41	1.56	0.39	0.35	0.28	0.06	0.02	1.14	0.07
		σ		0.3	0.93	0.09	0.00	0.02	0.00	0.00	0.00	0.01	0.27	0.01
Oudenburg	Sb	μ	7	71.1	18.23	5.79	1.84	0.38	0.44	0.35	0.06	0.02	0.48	0.02
		σ		1.7	0.61	0.76	0.15	0.05	0.17	0.08	0.01	0.01	0.13	0.01
	Mn and Sb	μ	36	69.0	18.17	6.73	2.18	0.58	0.61	0.58	0.09	0.37	0.34	0.07
		σ		0.9	0.75	0.44	0.19	0.20	0.16	0.16	0.02	0.19	0.09	0.04
	HIMT	μ	11	66.1	18.83	6.43	2.54	0.44	0.93	1.29	0.30	1.74	0.01	0.06
		σ		0.9	0.54	0.42	0.10	0.08	0.05	0.17	0.04	0.15	0.01	0.02
	Mn	μ	5	69.3	14.43	8.64	2.96	0.44	0.60	0.55	0.07	1.68	0.01	0.10
		σ		0.9	1.45	0.86	0.28	0.13	0.09	0.17	0.01	0.14	0.01	0.02
	Fe alone		1	71.0	17.26	6.51	2.01	0.30	0.74	0.55	0.11	0.09	0.001	0.02
Iulia Felix	Cl2 Mn	μ	9	70.3	14.96	7.87	2.55	0.52	0.59	0.16	0.07	1.42	< 0.03	0.15
		σ		0.9	0.48	0.32	0.12	0.08	0.10	0.15	0.01	0.21		0.05
	Cl1/2 Mn and Sb	μ	7	68.9	18.61	6.29	2.28	0.53	0.64	0.61	0.12	0.21	0.73	0.08
		σ		0.6	0.48	0.26	0.10	0.06	0.10	0.13	0.03	0.12	0.22	0.02
	Cl1 Sb	μ	28	70.3	19.84	4.74	1.93	0.39	0.29	0.33	0.06	< 0.01	0.86	0.02
		σ		0.4	0.43	0.18	0.07	0.04	0.06	0.03	0.01		0.10	0.005
	Ic1b Mn and Sb	μ	21	69.8	17.61	6.43	2.28	0.57	0.58	0.47	0.10	0.37	0.43	0.11
		σ		0.4	0.28	0.22	0.06	0.02	0.04	0.04	0.01	0.05	0.08	0.01
	Ic2b Mn	μ	3	68.6	16.59	7.65	2.37	0.80	0.88	0.55	0.10	0.82	0.12	0.25
		σ		1.4	0.92	0.15	0.07	0.16	0.40	0.12	0.03	0.13	0.21	0.13
	Ic1a Mn	μ	11	70.1	16.63	6.94	2.43	0.69	0.62	0.47	0.09	0.48	0.08	0.18
		σ		0.5	0.46	0.33	0.06	0.07	0.04	0.06	0.01	0.05	0.12	0.03
	Ic2a Mn	μ	15	70.4	16.07	7.83	2.55	0.49	0.53	0.34	0.07	0.37	< 0.03	0.13
		σ		0.6	0.66	0.37	0.08	0.06	0.07	0.07	0.01	0.11		0.02
Purple	purple	μ	6	65.8	17.09	7.90	2.38	0.67	0.80	0.81	0.10	1.96	0.05	0.11
		σ		1.4	1.09	0.36	0.10	0.13	0.27	0.35	0.05	0.28	0.08	0.01
Adria	AD/N2 Sb	μ	3	69.2	18.84	5.44	1.87	0.46	0.51	0.40	0.08	0.09	0.53	0.04
		σ		1.1	0.27	0.09	0.23	0.08	0.07	0.12	0.02	0.08	0.07	0.02
Reference				70.2	17.00	8.80	2.48	0.64	0.57	n.a.	n.a.	n.a.	n.a.	n.a.

2.2. Analytical methods

Glass samples were analysed by means of Ultraviolet-visible-Near Infrared (UV-vis-NIR) spectroscopy. Before performing optical analyses, a surface area (approximatively 5 x 5 mm^2) of each sample was

polished, using a hand-held Dremel® 3000 rotary tool, in order to guarantee maximum transmittance. Samples were illuminated using two lamps as light sources, a 30 W deuterium lamp for the UV spectral region and a 20 W halogen lamp emitting in the visible and infrared regions. Optical fibres guided light from the lamps to a plano-convex lens, which focused the emitted light to a spot size of around 3 mm in diameter at the position of the sample. The transmitted light was collected in an integrating sphere with an aperture of 6 mm, which was connected via optical fibres to two optical spectrometers, the AvaSpec-3648 and the AvaSpec-256- NIR1.7 from Avantes (Meulebroeck et al. 2010; Ceglia et al. 2015b), allowing the recording of the transmittance spectra between 250–1650 nm with a spectral resolution of 1 nm. Absorbance spectra were than calculated by means of $A=\log_{10}((1-R)^2/T)$ with R= reflectance and T= transmittance.

Fresnel reflection losses at the surface were taken into account, considering that the incident angle did not exceed 20° and that the glass refractive index was 1.5, so that the reflectance was 4% for each surface (Bamford 1977; Ceglia et al. 2015b).

Using Beer-Lambert's law ($A = \epsilon\, c\, l$ where c is the concentration of the absorbing species, ϵ is the molar attenuation coefficient and l the sample thickness), the absorbance can be directly related to the concentration of a species, if the thickness and the extinction coefficients are known. In soda-lime silicate glasses, the average extinction coefficient was determined experimentally, for Fe^{2+} at 1100 nm, to be 27.5±1.5 $L \cdot mol^{-1} \cdot cm^{-1}$, assuming a density of 2.5 g cm^{-3} (Ceglia et al. 2015b).

Once the absorbance spectra of the samples were obtained, they were normalised to a sample of 1 mm thickness, as a result of accurate and precise measurement of the samples thickness with a resolution of 0.001 mm beforehand by using a digital micrometre. The spectra were also modelled for different thicknesses (2, 5, 10, 15, 20 mm), using the Beer-Lambert's law.

The optical spectra were used to determine the colour coordinates and the iron redox ratio. The CIE Lab 1976 colour system with the standard illuminant D65 (L*, a*, b*) was used because of its advantage to quantifying colour in a linear Cartesian system, which could be compared with other analyses of glass colour (Alberghina et al., 2014; Ceglia et al., 2016; Maltoni and Silvestri, 2018; Silvestri et al., 2015, 2014, 2012).

We used Euclidian distances ΔE, defined in Equation 1, between two sets of colour coordinates (L_1^*, a_1^*, b_1^*) and (L_2^*, a_2^*, b_2^*) to quantitatively assess and compare glass colours (Marcus 1998).

$$\Delta E = \sqrt{(L_1^* - L_2^*)^2 + (a_1^* - a_2^*)^2 + (b_1^* - b_2^*)^2} \qquad \text{Equation 1}$$

Based on colour theories, it can be considered that:

- if ΔE is ≤ 2.3, the difference in colour is defined as 'just noticeable' (Sharma and Bala 2003; Ceglia et al. 2016);
- if ΔE is between 2.3 and 3.5, a small difference in colour is noticed by an unexperienced observer (Mokrzycki and Tatol 2011);
- if ΔE is between 3.5 and 5, a clear difference in colour is noticed (Mokrzycki and Tatol 2011); and
- if ΔE is > 5, two colours are considered different by observers (Mokrzycki and Tatol 2011).

In the present study, ΔE between colour coordinates of archaeological samples and that of the reference glass, containing no colouring or decolouring agents, is calculated to determine which glass of the studied assemblage was actually colourless.

The ferrous amount was determined following a well-established method that relies on the use of Beer-Lambert law, knowing that Fe^{2+} absorbs at 1100 nm in soda-lime silica glass (Weyl 1951; Bamford 1977; Möncke et al. 2014; Ceglia et al. 2016). In particular, the calibration curve established by Ceglia et al. (2015b) was used, to determine the ferrous concentrations. It should be stressed that, in order to validate the calibration curve, Ceglia et al. (2015b) compared results obtained by means of optical absorption spectroscopy with those by XANES spectroscopy, one of the most powerful, flexible and non-destructive methods to study the redox state of elements in historical glass research (e.g., (Quartieri and Arletti 2013)). Optical absorption spectroscopy gave nearly the same results as XANES, evidenced by a good correlation coefficient (r^2= 0.961) and the closely matched results between the above two techniques, which justified our use of UV-vis-NIR spectroscopy as an analytical method to determine quantitative data on Fe^{2+} contents in glass samples of the present assemblage. Following Ceglia et al. (2015b), the main source of error on the ferrous iron concentration is the error on the thickness measurement of the archaeological glass samples, which was estimated to be a maximum 0.1 mm of the actual value. The ferrous concentration of samples thicker and thinner by 0.1 mm was thus also calculated and used to determine the error on the total ferrous concentration of a sample. Error on the total concentration of iron was also taken into account as reported in the literature (Silvestri et al. 2008, 2014; Silvestri 2008; Ganio et al. 2012; Gallo et al. 2013; Mendera et al. 2017; Bidegaray et al. 2019).

3. Results and discussion

The absorbance spectra of glass samples representative of various compositional groups considered here (Sb-, Mn-, Mn-Sb, Purple, HIMT, and Fe alone) are shown in Figure 1. The colour coordinates are given in the tables and the colour background of each row of tables correspond to the glass calculated by means of (Colorizer 2018) on the basis of specific L*, a* and b* of that glass. The absorbance spectra of Figure 1a are due to glasses with similar amounts of iron (around 0.5 wt% Fe_2O_3) with or without manganese and antimony and are representative of compositional groups Fe-alone, Sb- and Mn and Sb glass. The glass with only iron (Fe alone) has the strongest absorption peak of Fe^{2+} at 1100 nm. The absorption peak is the smallest for the glass containing only antimony. When the two decolouring agents (antimony and manganese) are present together with iron, the absorption peak is intermediate. Figure 1b shows the absorbance spectra of glasses that contain the same amount of manganese (1.54 wt% MnO), but have very distinctive colours, as testified by colour coordinates reported in the corresponding Table. The selected samples are representative of compositional groups Purple, HIMT and Mn-glass. The purple glass has a strong absorption peak at 490 nm, caused by the presence of the chromophore Mn^{3+}. HIMT glass has much higher concentrations of Fe_2O_3 than the other glasses (1.1 wt% Fe_2O_3 for HIMT, whereas there is only 0.4 wt% Fe_2O_3 for the two other samples), leading to a stronger saturation of the colour. For comparative purpose and to emphasise the small but crucial variations in the optical absorption, due to the subtle balance between $Fe^{2+}/Fe^{3+}/Mn^{3+}$, the absorbance spectra as a function of wavenumbers (cm^{-1}) of all the samples, considered into Figures 1a-b, were also reported on the same plot (Figure 1c).

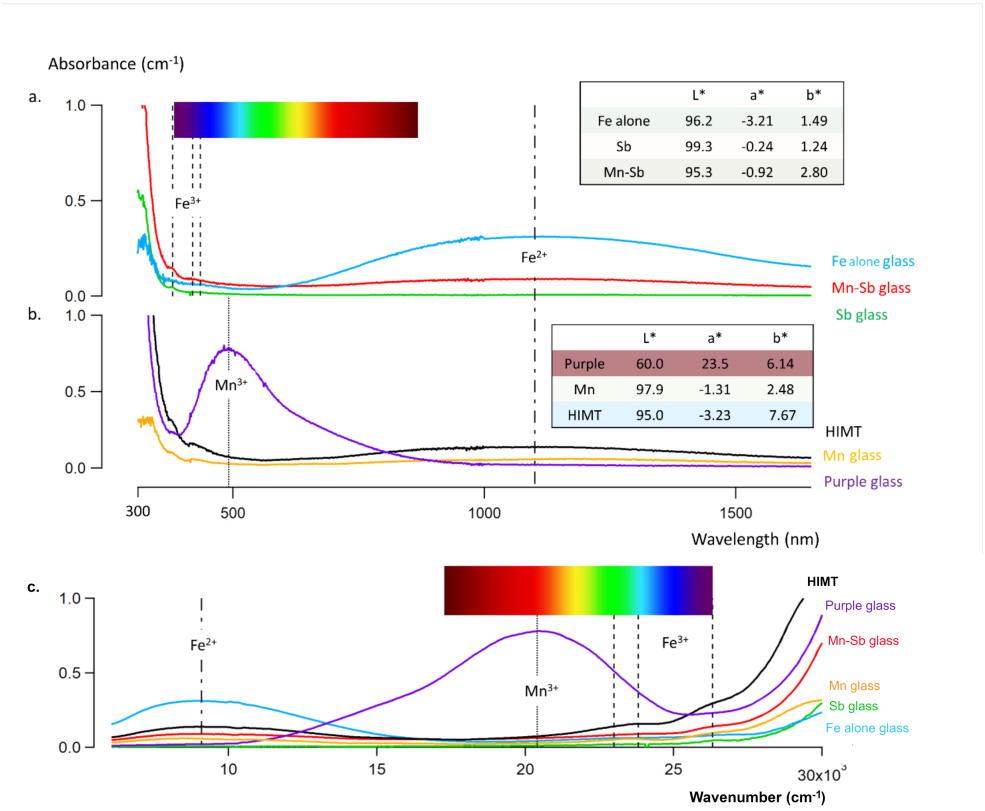

***Figure 1**. Absorbance as a function of wavelength normalised to 1 mm for different compositional groups; **a.** Glass containing similar amounts of Fe_2O_3 with or without antimony and manganese (Fe alone: OU9_5b, Sb-glass: IFB_5 and Mn-glass: IFC_30, respectively), **b.** Glasses having 1.54 wt% of MnO but very different colours: purple (ADV_3) and Mn-glass (OU9_9) have similar Fe_2O_3 concentrations (equal to 0.4 wt%), HIMT (OU6_2) has 1.1 wt% Fe_2O_3. The tables give the colour coordinates and the apparent colour (see colour background of each row). Visible range is also marked; **c.** Absorbance as a function of wavenumber (cm-1) normalised to 1 mm for all the glass samples considered in figures 1a-b.*

The normalised reference glass produced without any colouring or decolouring agents has colour coordinates L*, a*, and b* equal to 96.9, -0.11, and 1.14, respectively. The Euclidian distance, defined in Equation 1, between the colour coordinates of each archaeological sample and that of the normalised reference glass was calculated to determine which glass of the studied assemblage was colourless. An archaeological sample can therefore be considered as a colourless glass, if it would have colour coordinates such as $\sqrt{(L^* - 96.9)^2 + (a^* + 0.11)^2 + (b^* - 1.14)^2} \leq 2.3$. The ΔE values, below the threshold of 2.3, are marked in green in Appendix.

3.1. To what extent does glass thickness influence colour?

In order to understand the influence of thickness on glass colour and to answer the question of what colourless means for glass, absorbance spectra were modelled for different thicknesses. All the colour coordinates for the different modelled thicknesses, as well as the ferrous iron concentrations of the glasses analysed, are reported in Appendix. Figure 2 gives some examples of absorbance spectra of analysed samples (i.e., Sb-glass, IFP_2, Purple glass, ADV_3, and HIMT glass, OU6_4) at different thicknesses (i.e., original thicknesses equal to 2.476, 1.039, and 3.487 mm for IFP_2, ADV_3, and OU6_4, respectively, and modelled at 1, 2, 5, 10, 15 and 20 mm). It was observed that the thicker the glass, the less light was transmitted in the visible range.

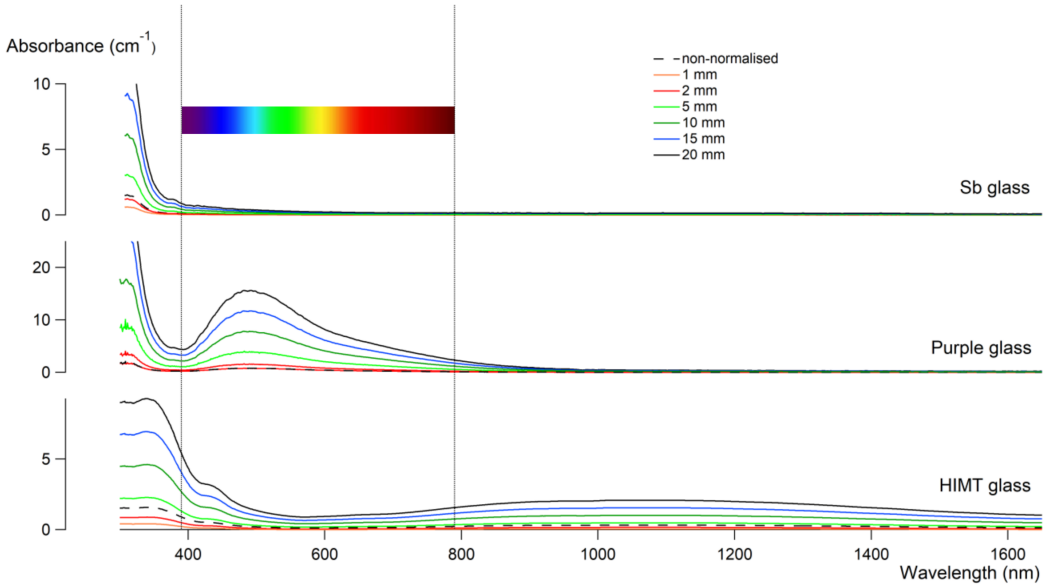

Figure 2. *Absorbance as a function of wavelength for three glasses modelled at different thicknesses (non-normalised corresponds to original thickness). Visible range is also marked. The thicker the glass becomes; the less light is transmitted.*

Therefore, it is necessary to differentiate 'intrinsic' from 'perceived' colour of a glass. In the present study, we consider the 'perceived' colour as the colour coordinates and appearance of a sample with its original thickness, whereas the 'intrinsic' colour is the colour of that sample if thickness is normalised to 1 mm.

Overall, only eight non-normalised samples (i.e., samples with their original thickness) could be considered colourless (i.e., $\Delta E < 2.3$), whereas 138 of the normalised samples (i.e., samples with thickness normalised to 1 mm) were colourless (samples marked in green into Appendix). This implies that the variability in the thickness of the glass object can cause an important bias when archaeological glass is classified according to the perception of colour by the naked eye, as also remarked by (Ceglia et al. 2016; Gliozzo 2017).

Thickness can even cause a glass to appear coloured, even though it would be considered colourless if it was thinner. For instance, IFP_23, an antimony decoloured glass, showed a yellowish hue (ΔE = 13.8) with its original thickness (4.185 mm), but it would be colourless (ΔE = 0.48) if the thickness was normalised to 1 mm (see Appendix, line no. 53).

3.2. How does iron redox affect the glass colour?

A logical question that emanates from the previous discussion is how iron redox changes affect glass colour. In this respect, it is useful to analyse how colour coordinates (in particular, parameters a* and b*) are related to the concentrations of ferrous iron in normalised samples, as shown in Figure 3.

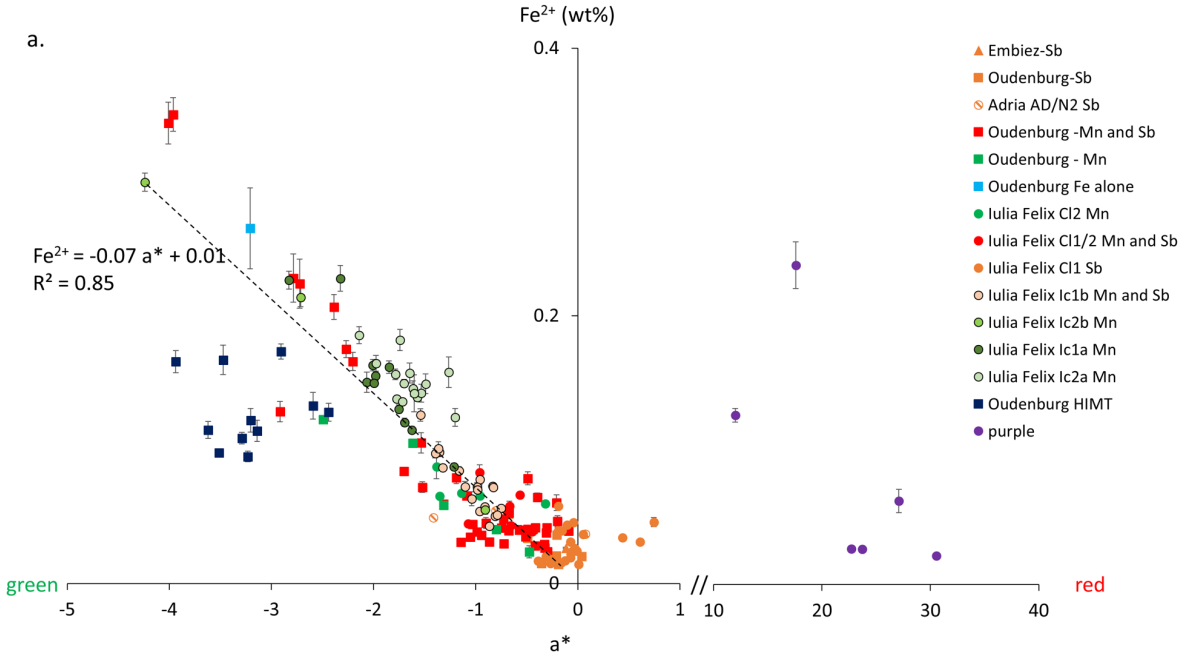

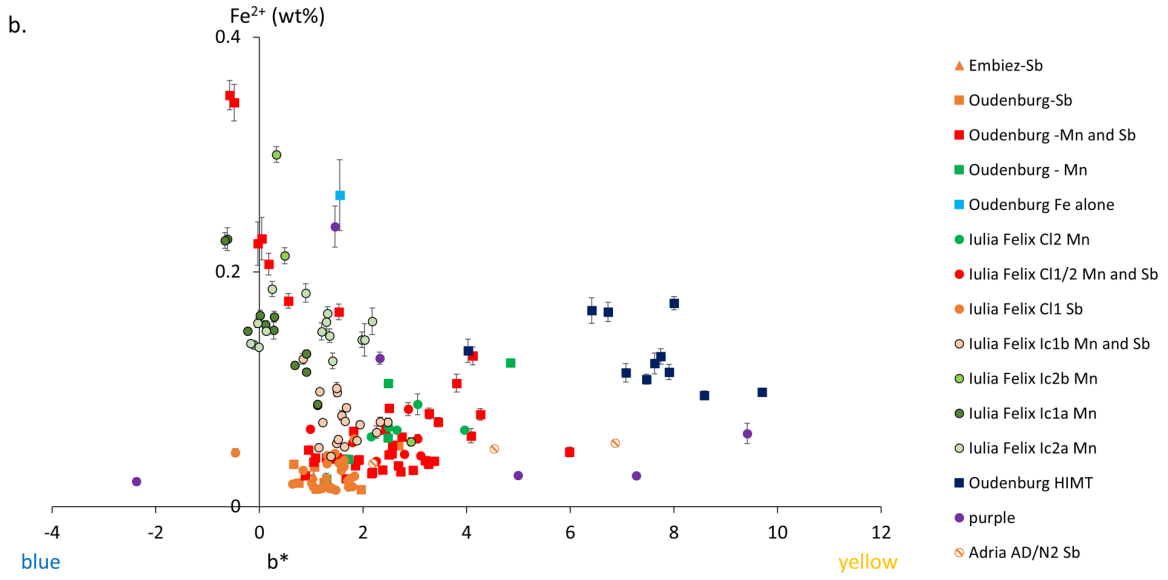

Figure 3. *In samples with thickness normalised to 1 mm, the total amounts of ferrous iron (wt%):* ***a****. as a function of a*, where it seems to be a correlation for all samples, apart from purple and HIMT glass;* ***b.*** *as a function of b* without a correlation.* The shapes of the symbols correspond to provenance (Italian glasses are represented by circles, Oudenburg glass by squares and Embiez glass by triangles), and the colours of the symbols correspond to compositional groups (light blue: Fe-alone; orange: Sb-glass; green: Mn-glass; red and pink: Mn and Sb glass; dark blue: HIMT glass; purple: purple glass).

It can be observed in Figure 3a that the more ferrous iron there is, the more negative the a* value will be, thus the greener the glass appears, as expected from the extensive literature on the subject (Bamford 1977; Paul 1982). Although there seems to be a correlation between Fe^{2+} and a* for all groups, except for HIMT and purple glass (R^2 = 0.85), one should be particularly careful and draw immediate conclusions. Several authors (e.g., (Vercamer et al. 2015)) have studied this and no immediate correlation exists. In the case of purple glass, the absence of correlation between Fe^{2+} and a* is probably due to Mn^{3+}, which acts as a strong chromophore (the molar extinction coefficient of Mn^{3+} is 25-100 L cm^{-1} mol^{-1}, which is higher than those of Fe^{2+}, also known for its strong colouring power (about 30-54 L cm^{-1} mol^{-1}), and Fe^{3+} (about 3-5 L cm^{-1} mol^{-1}), in accordance with data reported into Table 2 of (Möncke et al. 2014)) and plays, therefore, a crucial role in determining final colour. For HIMT, the discrepancy from the linear correlation between Fe^{2+} and a* can be explained by the high iron and manganese contents (Fe_2O_3 = 1.29 ± 0.18 wt% and MnO = 1.74 ± 0.15 wt%, respectively), and the HIMT glasses of the present assemblage are the samples with much more intense unintentional colours (higher a* and b* than those measured in other unintentionally coloured samples, as evident in Figure 3).

Such a correlation was not noticed between Fe^{2+} and the colour coordinate b* (Figure 3b).

Colour is a complex function, depending not only on the total amount of iron and its redox ratio but also on the concentration and redox state of other multivalent elements, such as manganese and

antimony. The relationships between iron redox and manganese/antimony contents and between manganese/antimony contents and glass colour of the present assemblage are, therefore, discussed in next two sub-sections.

3.3 To what extent do manganese/antimony contents influence iron redox?

Mutual redox reactions occur between different multivalent elements (Borisov, 2016; Kido et al., 2005; Schreiber et al., 1996) as described in Equation 2.

$$Fe^{2+} + Mn^{3+} \leftrightharpoons Fe^{3+} + Mn^{2+}$$

$$2\,Fe^{2+} + Sb^{5+} \leftrightharpoons 2\,Fe^{3+} + Sb^{3+}$$

Equation 2

Archaeometric studies on glass suggest that antimony is a more effective oxidising agent than manganese e.g., (Jackson 2005; Arletti et al. 2013). Some materials scientists on the other hand conclude the opposite for glass with similar chemical compositions: manganese has been considered as more efficient than antimony on the basis of electromotive force series calculations and experimental verifications for soda-lime silica glass containing 1 wt% of iron (e.g., (Schreiber et al. 1999; Donald et al. 2006). The difficulty in determining which is the most efficient oxidising agent comes from the exchange of two electrons in the case of antimony, which makes it more sensitive to the partial oxygen pressure within the melt, as described by Bingham and Jackson (2008). Furthermore, it is possible that antimony and manganese can react with themselves (Donald et al. 2006).

It is expected that the more oxidising agent there is, the less reduced the glass will be, i.e., for a given concentration, the higher the proportion of reduced iron, the lower the proportion of oxidised iron. To verify this, Figure 4 shows the redox ratio of iron (Fe^{2+}/Fe_{tot}) as a function of the ratio of the decolouring agents to iron [(Mn+Sb/2)/Fe] given in mol%. The ratio [(Mn+Sb/2)/Fe] was calculated using molar concentrations of the decolouring agent and takes into account the stoichiometry of Equation 2 (i.e., theoretically one mole of antimony is necessary to oxidise two moles of iron, whereas one mole of manganese would oxidise one mole of iron). A ratio equal to 1 represents stoichiometric proportions, whereas oxidising agents are in excess or in defect for a ratio above or below 1, respectively.

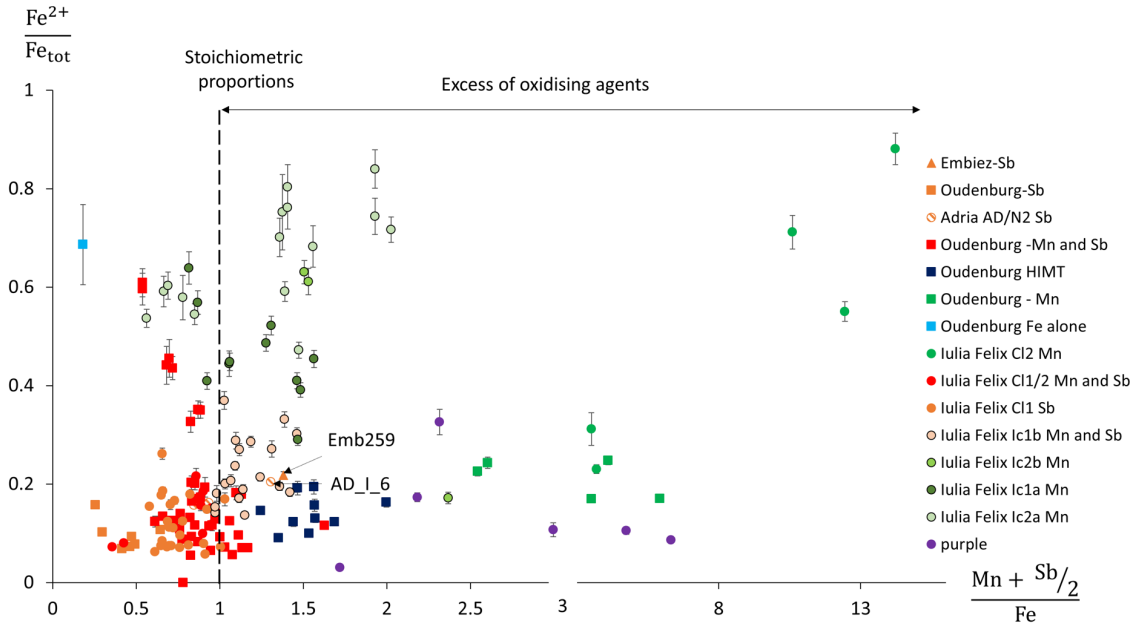

Figure 4. *Redox ratio (Fe^{2+}/Fe_{tot}) as a function of the molar ratio of decolouring agents towards iron [(Mn+Sb/2)/Fe]. The shapes of the symbols correspond to provenance (Italian glasses are represented by circles, Oudenburg glass by squares and Embiez glass by triangles), and the colours of the symbols correspond to compositional groups (light blue: Fe-alone; orange: Sb-glass; green: Mn-glass; red and pink: Mn and Sb glass; dark blue: HIMT glass; purple: purple glass). The error bars are calculated as described in section 2.1. Some error bars are smaller than the data points. Note that antimony is never in excess, even though the iron is quite oxidised, whereas manganese can be present in large excesses and does not necessarily lead to full iron oxidation.*

First, it can be observed in Figure 4 that most of the data points are close to stoichiometric proportions (122 samples over a total of 166 show stoichiometric proportions between 0.5 and 1.5 and, among these, 33 have values between 0.9 and 1.1), whereas there are some isolated points (18 samples) corresponding to glass with large excesses of oxidising agent (with a ratio above 2). Moreover, no link between the amount of decolouring agent and the iron redox ratio is clearly visible on Figure 4, when considering the data set as a whole, but some trends are identified within different glass groups.

Sample “Fe alone” (light blue data point in Figure 4) shows a redox ratio equal to 0.68 ± 0.08, which corresponds quite well to the average value (0.60 ± 0.15) measured in prior work on late antique naturally coloured glass, with only iron as chromophore and no decolourisers, which was classified as Levantine 1 (Ceglia et al. 2016).

Sb glass (orange data points in Fig. 4) never has antimony in molar excess, apart from one sample from the Embiez (Emb_0259) and one from Adria (AD_I_6) that are above stoichiometric proportions. Sb glass is also the most oxidised with iron redox ratios between 0.06 and 0.26. This suggests that antimony could be a very efficient oxidising agent. Apart from interacting directly with iron following Equation 2, antimony also acts as a fining agent, so that it helps to remove bubbles and dissolved gases from the melt as shown in Equation 3.

$$Sb_2O_5\ (melt) \leftrightharpoons Sb_2O_3\ (melt) + O_2\ (gas) \qquad \text{Equation 3}$$

Bigger bubbles containing oxygen are thus produced, which rise to the surface by buoyancy, thus leading to a glass with less undesirable bubbles (Shelby 2005; Müller-Simon 2011). The release of these bubbles could also oxidise iron. Antimony thus not only oxidises iron in a direct way (Equation 2) but the same effect could also be obtained in an indirect way through the release of bubbles, although this last hypothesis needs additional studies to be experimentally verified.

Describing Mn glass (green data points in Fig. 4) is more complex, as samples show a large variability. Mn glass samples, considered to be macroscopically colourless, typically have a very high excess of manganese (MnO/Fe_2O_3 ratios are all above 3). This is in line with results obtained on a little selection of Roman and Medieval glass by Silvestri et al. (2005), who conclude that manganese acts as an effective decolourant, if the ratio MnO/Fe_2O_3 is >2. However, some glasses from this group have very high redox ratios. This is due to the fact that these glasses have relatively low concentrations of the total iron content (less than 0.15 wt% Fe_2O_3), but their ferrous iron concentrations are similar to those of other Mn glasses and have a higher total iron content. The same goes for glasses that contain only manganese as a decolouring agent but which were classified as naturally coloured instead of colourless glass (*Iulia Felix* groups Ic1a, Ic2a, and Ic2b).

It is interesting to note that glasses containing both antimony and manganese (red and pink data points in Fig. 4) do not have an excess of oxidising agents, unlike the manganese containing glass group, but in the same way as antimony glass. It is generally considered that the presence of both decolouring agents comes from recycling, the so-called 'great melting pot' (Freestone 2015; Jackson and Paynter 2015; Paynter and Jackson 2016).

HIMT and purple glass samples (dark blue and purple data points in Figure 4) show distinctive characteristics. HIMT glass is a separate case, both due to its different archaeological context, as it was used only from the 4th century onwards, and to its chemical composition, in that it has much higher iron contents than other glass considered here. Yet, HIMT samples do not show a large excess of manganese compared to iron (the molar ratio of decolouring agent towards iron is less than 2), their redox ratios are relatively small, implying that HIMT glass is quite oxidised. This was also noticed in HIMT samples from Cyprus, where there is not necessarily a big excess of manganese, yet the glasses are quite oxidised (Ceglia et al. 2015a). For example, in HIMTb glass from Cyprus, the MnO/Fe_2O_3 ratio is only 0.47, whereas the redox ratio is 0.09 ± 0.01. In the case of purple glass, the iron is also quite oxidised (Fe^{2+}/Fe_{tot} less than 0.3), while there is a large excess of manganese (i.e. at least twice more manganese than iron).

To analyse furtherly trends, shown in Figure 4, that similar amounts of oxidising agents do not yield the same iron redox ratio, it is necessary to discuss thermodynamic and kinetic aspects of redox reactions in glass-forming melts. When there is only one multivalent element M, such as iron, in a silicate melt, it is in equilibrium with the physically dissolved oxygen (Schreiber 1986; Kress and Carmichael 1988). The general redox equation of multivalent element M, where n electrons are exchanged between the two different valent states, is given in Equation 4:

$$M^{x+} + n/2\ O_2 \leftrightharpoons M^{(n+x)+} + n/2\ O_2^{-} \qquad \text{Equation 4}$$

There is currently no consensus regarding what happens if another multivalent element is present. While certain researchers argue that redox reactions can occur at melt temperatures (Schreiber 1986; Schreiber et al. 1987; Cicconi et al. 2015), others maintain that mutual interactions between different multivalent elements occur during the cooling of the glass melt, because the system becomes closed to oxygen (Borisov, 2016; Rüssel, 2005, 1989). Melting temperatures and thermal treatments have an important influence on the final redox ratios. As a result, there can be variation in the redox ratios of glasses with similar contents of oxidising agents due to distinctive production events, where different thermal treatments were applied. This could be one element explaining the lack of correlation in Figure 4. Alternatively, as suggested by Bingham and Jackson (2008), it is possible that redox equilibria with the atmosphere were not necessarily reached. Another hypothesis is related to the concept of 'redox number' introduced for the glass industry by Simpson and Myers (1978), who empirically attributed a redox value to different raw materials based on their influences on the redox ratio of the glass batch. This concept is used commonly nowadays in the glass industry, where the same furnace tank can be used to produce glass in different colours based on changes in the raw materials rather than on temperature and atmosphere modifications (Chopinet et al. 2002; Biron and Chopinet 2013). Consequently, it would be possible that Roman glassmakers added different raw materials or that a source of carbon, such as charcoal, would have been added during the melting process, thus influencing the redox number of the batch and, hence, the final glass colour

(Simpson and Myers 1978; Iyel et al. 2014).

3.4 What is the link between manganese/antimony contents and glass colour?

To look at the relation between manganese/antimony contents and glass colour, samples from different provenances have been grouped together based on the presence or absence of the decolouring agents (antimony and manganese). The average chemical compositions, as well as redox ratios and normalised colour coordinates of groups Sb, Mn-Sb, Mn, and HIMT, are reported in **Table 2**.

Table 2. *Average (μ) chemical composition (in wt%) and standard deviation (σ) of the four compositional groups considered here (Sb, Mn-Sb, Mn, HIMT), as well as average (μ) and standard deviation (σ) of colour coordinates for normalised samples and the redox ratios; n: number of samples for each group.*

group	n		SiO_2	Na_2O	CaO	Al_2O_3	K_2O	MgO	Fe_2O_3	TiO_2	MnO	Sb_2O_3	L*	a*	b*	Fe^{2+}/Fe_{tot}
Sb	40	μ	70.4	19.43	5.03	1.89	0.39	0.34	0.34	0.06	0.02	0.78	97.2	-0.16	1.59	0.12
		σ	0.9	0.8	0.56	0.13	0.04	0.12	0.06	0.01	0.03	0.22	2.76	0.36	1.15	0.05
Mn-Sb	64	μ	69.2	18.05	6.59	2.22	0.57	0.6	0.55	0.09	0.35	0.41	97.3	-1.02	1.93	0.18
		σ	0.8	0.69	0.4	0.16	0.15	0.13	0.14	0.02	0.16	0.16	1.32	0.75	0.99	0.12
Mn	43	μ	70.1	15.83	7.69	2.55	0.56	0.6	0.37	0.08	0.8	0.04	96.7	-1.69	1.21	0.51
		σ	0.9	1.05	0.66	0.2	0.14	0.14	0.17	0.01	0.53	0.08	1.19	0.68	1.27	0.2
HIMT	11	μ	66.1	18.83	6.43	2.54	0.44	0.93	1.29	0.3	1.74	0.01	94.5	-3.21	7.39	0.15
		σ	0.9	0.54	0.42	0.1	0.08	0.05	0.17	0.04	0.15	0.01	2.58	0.44	1.43	0.03

In Figure 5, the box plots are given for the colour coordinates (L*, a*, b*) and ΔE of four compositional groups at a thickness of 1 mm (normalised) and 10 mm, to further demonstrate (see also section 3.1) thickness has a crucial influence on glass colour and, therefore, has to be considered a key parameter when comparing colours of different chemical composition groups. It can be observed that Sb glass has the highest L* but the lowest a*, b* and ΔE and is thus always the closest to be colourless; whereas, HIMT glass has the highest ΔE and b* and lowest L*, making it the most coloured. Mn-Sb glass is intermediate with values of a* and L*, between that of Mn glass and Sb glass (Figure 5).

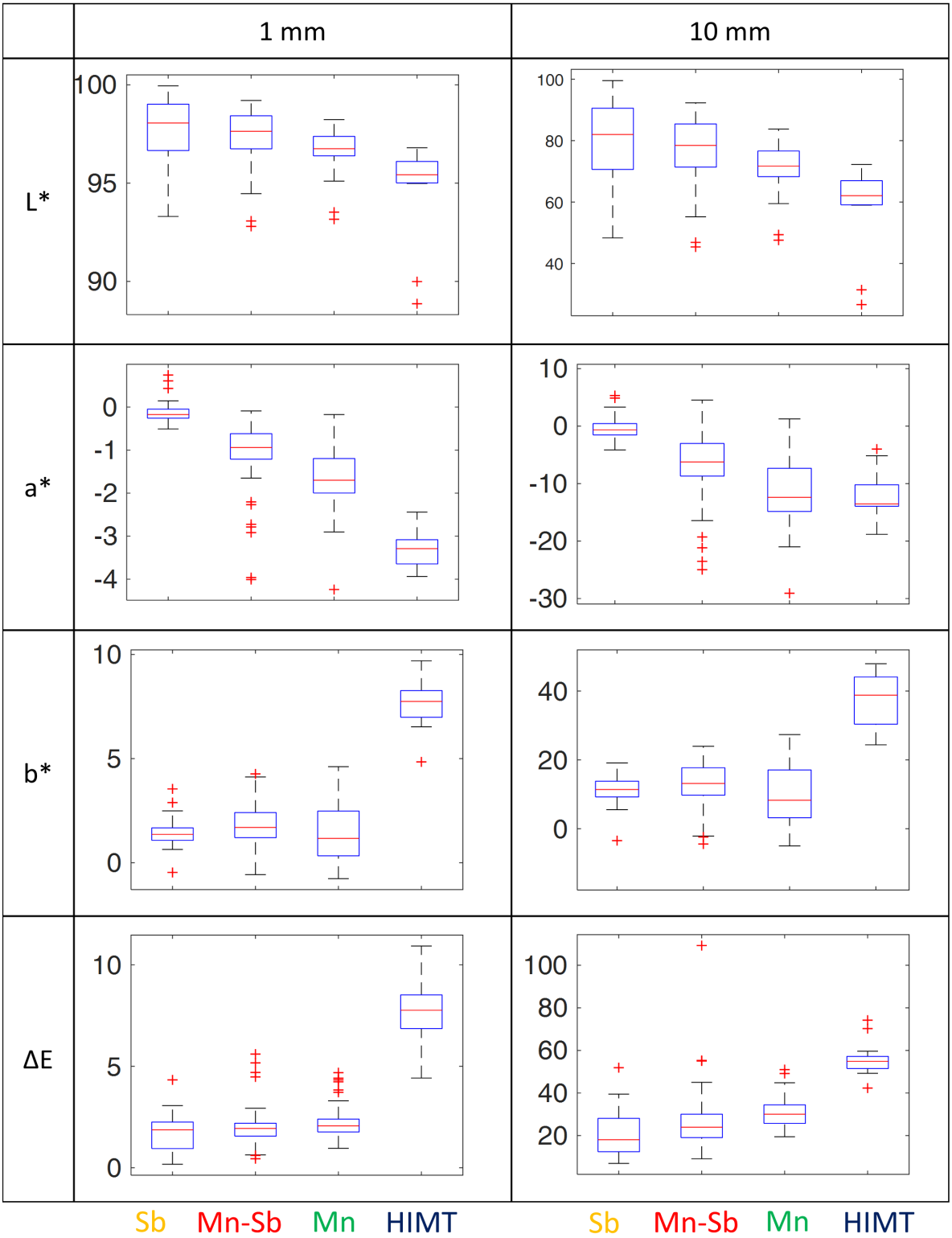

Figure 5. *Box plots giving the colour coordinates (L*, a*, b*) and ΔE of Sb, Mn-Sb, Mn and HIMT glass groups, modelled for thicknesses of 1 and 10 mm. Medians are shown as a red line within each box; the boxes are limited by the first and third quartiles, while the maxima and minima are represented by the extremes of the dotted lines. Outliers are also represented as isolated red crosses.*

After looking at the possible variability within each compositional group using the box plots of Figure 5, samples with median colour coordinates (IFB_26 for Mn glass, IFP_2 for Sb glass, IFB_85 for Mn-Sb glass and OU9_7 for HIMT) and sample Fe alone were chosen, in order to discuss the influence of glass thickness on ΔE and the evolution of L* (lightness factor) as a function of a* and b* at six thicknesses (1, 2, 5, 10, 15, and 20 mm), and at original thickness for each sample. ΔE and L* are, in fact, two important factors as the first allows us to differentiate "intrinsic" from "perceived" colour of glass, and to estimate how "colourless" is a glass, and the second is related to how much light goes through the material.

Figure 6a shows how ΔE varies with glass thickness; in this figure, sample ADV_3 as representative of purple glass is also considered. In general, from the figure it is evident that ΔE increases with increasing thickness, and the difference between intrinsic and perceived colours is dependent from the original thickness of the sample. For instance, in the case of purple glass shown in Figure 6a (ADV_3), the sample was not very thick (1.039 mm), so there was only a slight difference between the normalised to 1 mm and non-normalised spectra (L* a* b* = 60.01, 23.48, 6.14 vs 56.81, 23.34, 6.10, respectively), and, consequently, between the intrinsic and perceived colours (ΔE = 44.07 vs 46.71, respectively). The larger thickness of Sb glass, shown in Figure 6a (IFP_2 with thickness of 2.476 mm), caused an increased difference between its perceived and intrinsic colour, having colour coordinates L* a* b* equal to 93.80, -0.26, 4.03 vs 98.71, -.013, 1.71, and a ΔE of 4.24 vs 1.90, respectively. As the Mn-glass, shown in Figure 6a, was much thicker (IFB_26 with thickness of 3.562 mm) than the others, its intrinsic and perceived colours were even more different: the sample with its original thickness has ΔE equal to 12.50, whereas it could be considered colourless, if thickness was normalised to 1 mm (ΔE = 1.66).

Figure 6b shows the variations of colour coordinates for all groups (Sb-, Mn-, Mn-Sb glass, HIMT and Fe alone, except for purple glass) at six thicknesses (1, 2, 5, 10, 15, and 20 mm), and at original thickness. In general, it can be observed the thicker the glass is, the further the colour coordinates are from the origin, and that there seems to be a linear relation in the evolution of the colour coordinates as thickness increases up to a certain point. This is very clear for HIMT glass, where linearity is lost when a* or b* reaches its highest value. The above linear relation can be directly related to the evolution of the optical spectra with increasing thickness as shown in Figure 2: as the glass becomes thicker, certain chromophores will prevail depending on their extinction coefficients, thus leading to a stronger absorption at specific wavelengths.

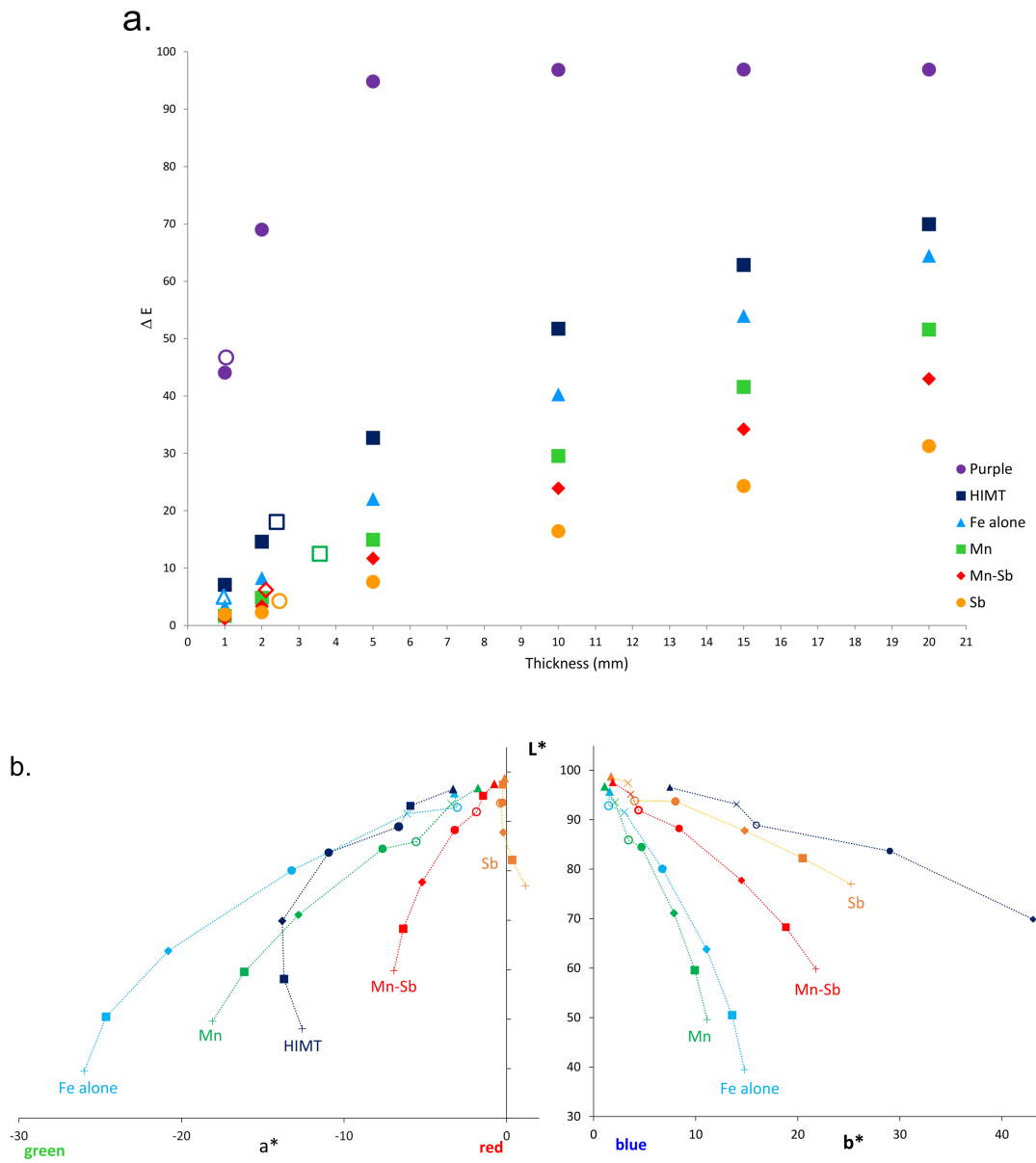

Figure 6. a.: *ΔE as a function of thickness for glasses representative of various compositional groups here considered. Note the increase of ΔE with increasing of thickness (empty symbols correspond to ΔE of non-normalised sample, i.e., with its original thickness). Selected samples are: IFP_2 (with original thickness of 2.476 mm) as representative of Sb glass, IFB_85 (with original thickness of 2.106 mm) as representative of Mn-Sb glass, IFB_26 (with original thickness of 3.562 mm) as representative of Mn glass, ADV_3 (with original thickness of 1.039 mm) as representative of purple glass, and OU7_2 (with original thickness of 2.224 mm), as representative of HIMT glass, as well as of sample Fe alone.* ***b:*** *Colour coordinates (L* as a function of a* on the left and L* as a function of b* on the right) for the above same samples characteristic of the different chemical compositional groups for six thicknesses (▲1, x 2, ● 5, ◆ 10, ■ 15, and + 20 mm) and for original thicknesses (empty circles), except for purple glass. Note that the thicker the glass is, the further from the origin the colour coordinates are.*

Figure 6b also demonstrates that colour coordinates of the different chemical compositional groups evolve differently in function of the thickness but, in any case, the thicker the glass, the higher a* and b* and the lower L* will be. Concerning sample "Fe alone", L* decreases most and a* becomes the most negative for increasing thicknesses. This means that, in the absence of decolouring agents,

596 thicker glass becomes greener and less light goes through. In contrast, the presence of antimony
597 dramatically limits the decrease of L* and the appearance of green colour in thick glass. Even at the
598 maximum thickness analysed here, the glass does not become green, but just gradually becomes
599 darker and more yellow (higher b*). Sb glass always has the highest values of L* compared to other
600 glass groups, meaning more light goes through antimony glass than any other glass group. Manganese
601 only slightly impedes glass becoming green, but its effect is rather limited compared to the sample "Fe
602 alone", which has no decolouring agents. Glass containing both manganese and antimony is
603 intermediate. The case of HIMT glass is again distinctive because of higher concentrations of both iron
604 and manganese. This is the reason why colour coordinates reach high values (b* even being the
605 highest) and illustrates again that, apart from redox state, the amount of multivalent elements plays a
606 key role in the definition of colour (Ceglia et al. 2016). Freestone et al. (2018) proposed that HIMT glass
607 would have been deliberately coloured for it to be differentiated from other glasses. This branding
608 strategy at the primary production level would have been carried out to indicate that HIMT glass was
609 easier to work.

610 An important caveat concerns the colour caused by manganese and antimony themselves. While
611 antimony contributes neither to the optical absorption spectrum nor to the glass colour whatever its
612 oxidation state, manganese has a stronger influence on the glass colour. Indeed, both Mn^{2+} and Mn^{3+}
613 have optical absorption bands (Mn^{2+} gives weak spin forbidden absorptions similar/overlapping with
614 Fe^{3+}; and Mn^{3+} gives an intense absorption as shown by the purple glass sample in Figure 1).

615 In this paper, the focus is on the influence of manganese and antimony on iron. It would thus appear
616 that antimony is the more effective decolouring agent, and its presence with manganese improves the
617 colour, and, consequently, glass quality, compared to that of a glass that would have been decoloured
618 only with manganese. Indeed, the mixing of greenish manganese glass with colourless antimony glass
619 results in a glass with an intermediate colour. Whatever the glass thickness, the a* parameter in Sb
620 glass is always much lower than that in Mn glass, thus meaning that antimony glass does not tend to
621 have the greenish colour typical of thicker manganese-containing glass. This result can be put in
622 parallel with the well-accepted hypothesis about the provenance of glass, proposing a Levantine
623 production of manganese glass (Foy 2000; Jackson and Paynter 2015) and an Egyptian production of
624 antimony glass (Gliozzo 2017; Schibille et al. 2017). Colour, quality, and provenance would thus be
625 quite in line with the Diocletian edict that classified Alexandrian (Egyptian) glass as colourless and
626 priced at 24 denarii a pound, whereas Judean (Levantine) glass is described as having a greenish colour
627 and priced at 13 denarii a pound (Whitehouse 2004; Freestone 2015). Although care should be taken
628 regarding the terminology and the extent to which the designation of a glass refers to its provenance
629 (Barag 2005), the data analysed here, by quantifying the colour improvement caused by the presence

of antimony, provide an additional argument in favour of antimony glass being more colourless (and therefore more high-quality and expensive) than manganese glass.

4. Conclusions

Based on a large dataset of Roman glass, the present study has critically evaluated interrelations among colour, thickness, iron redox, and manganese/antimony contents, by means of optical absorption spectroscopy, which allows us to determine concentrations of ferrous iron and colour coordinates. An objective method to evaluate colour is also proposed here and based on the Euclidian distances, ΔE, between colorimetric coordinates of archaeological samples and that of a reference colourless glass. This method was used to assess which glass samples of the present assemblage were, actually, colourless regardless of operator, and allowed us to highlight the importance of glass thickness. There is, in fact, a crucial difference between the 'intrinsic' glass colour (i.e., colour shown by a glass with thickness normalised to 1 mm) and the 'perceived' colour (i.e., colour of the glass with its original thickness).

In addition, this study has confirmed the important link between glass colour and iron redox ratio, because it has quantitatively proved there is a correlation between the colourimetric parameter a* and the total concentration of ferrous iron, apart from HIMT and purple glass. It should be stresses here that, although HIMT and purple glass behave differently, they also contain iron and manganese and have similar chemical compositions. For this reason, their analysis is intrinsically related to that of decoloured and other categories of unintentionally coloured glass. The authors hope, therefore, that the elements discussed here would encourage future research about the specific topic of manganese.

Furthermore, the study, by integrating optical and chemical data, allowed us to discuss relationships between manganese/antimony contents and iron redox ratio. Antimony appears to be a very efficient oxidising agent because it leads to the lowest iron redox ratios, while it was never in excess (i.e., the molar ratios [(Mn+Sb/2)/Fe] in Sb glass are lower than 1, value which represents stoichiometric proportions). Whatever the thickness of the glass, the presence of antimony drastically decreases the greenish colour in glass. In Mn glass (i.e., compositional groups Roman Mn-colourless and naturally coloured), the thicker the sample becomes, the greener the colour will be, and no correlation between the manganese amount and iron redox ratio could be detected. From the present analytical evidence, it can thus be hypothesised that antimony leads to the most oxidised and least greenish glass and, consequently, to a more colourless glass with respect to that containing manganese.

In conclusion, the present study clearly demonstrated (1) the optical absorption spectroscopy as a useful method to objectively and quantitatively evaluate the colour of historical glasses and (2) the necessity of thickness measurements when discussing glass colours, in order to make correct comparisons possible between quantified data, thereby enlarging the information deductible from samples of different periods and regions.

Acknowledgements

This research was supported by a PhD fellowship by the Research Foundation – Flanders (Fonds voor Wetenschappelijk Onderzoek, FWO), grant number 11Z8417N. We are very grateful to Sofie Vanhoutte from Agentschap Onroerend Erfgoed, Brussels, Belgium who gave access to the glass from Oudenburg and to Professor Patrick Degryse from Katholieke Universiteit Leuven for kindly making available the glass from the shipwreck of Ouest Embiez 1 he received from DRASSM, France. We would also like to thank Bart Lippens for the glass polishing.

References

Aerts A, Velde B, Janssens K, Dijkman W (2003) Change in silica sources in Roman and post-Roman glass. Spectrochim Acta Part B At Spectrosc 58:659–667. doi: 10.1016/S0584-8547(02)00287-2

Alberghina MF, Barraco R, Basile S, et al (2014) Mosaic floors of roman Villa del Casale: principal component analysis on spectrophotometric and colorimetric data. J Cult Herit 15:92–97. doi: 10.1016/j.culher.2012.12.004

Arletti R, Quartieri S, Freestone IC (2013) A XANES study of chromophores in archaeological glass. Appl Phys A 111:99–108. doi: 10.1007/s00339-012-7341-4

Arletti R, Vezzalini G, Benati S, et al (2010) Roman Window Glass: a Comparison of Findings From Three Different Italian Sites. Archaeometry 52:252–271. doi: 10.1111/j.1475-4754.2009.00479.x

Azzoni CB, Martino IDD, Marchesi V, et al (2005) COLOUR ATTRIBUTES OF MEDIEVAL WINDOW PANES: ELECTRON PARAMAGNETIC RESONANCE AND PROBE MICROANALYSES ON STAINED GLASS WINDOWS FROM PAVIA CARTHUSIAN MONASTERY*. Archaeometry 47:381–388. doi: 10.1111/j.1475-4754.2005.00208.x

Bamford CR (1977) Colour Generation and Control in Glass. Elsevier Scientific Publishing Company, Amsterdam-Oxford-NewYork

691 Barag D (2005) Alexandrian and Judaean Glass in the Price Edict of Diocletian. J Glass Stud 47:184–186

692 Bidegaray A-I, Ceglia A, Cicconi MR, et al (2018) An in-situ XANES investigation of the interactions
693 between iron, manganese and antimony in silicate melts. J Non Cryst Solids 502:227–235. doi:
694 https://doi.org/10.1016/j.jnoncrysol.2018.09.015

695 Bidegaray A-I, Cosyns P, Gratuze B, et al (2019) On the making, mixing and trading of glass from the
696 Roman military fort at Oudenburg (Belgium). Archaeol Anthropol Sci 11:2385–2405. doi:
697 10.1007/s12520-018-0680-0

698 Bingham PA, Jackson CM (2008) Roman blue-green bottle glass: chemical–optical analysis and high
699 temperature viscosity modelling. J Archaeol Sci 35:302–309. doi: 10.1016/j.jas.2007.03.011

700 Biron I, Chopinet M-H (2013) Colouring, Decolouring and Opacifying of Glass. In: Janssens K (ed)
701 Modern methods for analysing archaeological and historical glass. John Wiley & Sons Inc,
702 Chichester, West Sussex, United Kingdom, pp 49–65

703 Bonnerot O, Ceglia A, Michaelides D (2016) Technology and materials of Early Christian Cypriot wall
704 mosaics. J Archaeol Sci Reports 7:649–661. doi: 10.1016/J.JASREP.2015.10.019

705 Bonomi S (1996) Vetri antichi del Museo archeologico nazionale di Adria, Corpus delle Collezioni
706 archeologiche del Veneto, volume 2. Comitato nazionale italiano Association internazionale pour
707 l'histoire du verre, Venezia

708 Borisov AA (2016) Mutual interaction of redox pairs in silicate melts: Equilibria involving metallic
709 phases. Petrology 24:117–126. doi: 10.1134/S0869591116020028

710 Boschetti C, Henderson J, Evans J (2017) Mosaic tesserae from Italy and the production of
711 Mediterranean coloured glass (4th century BCE–4th century CE). Part II: Isotopic provenance. J
712 Archaeol Sci Reports 11:647–657. doi: 10.1016/j.jasrep.2016.12.032

713 Cagno S, Cosyns P, Izmer A, et al (2014) Deeply colored and black-appearing Roman glass: a continued
714 research. J Archaeol Sci 42:128–139. doi: 10.1016/j.jas.2013.11.003

715 Cagno S, Cosyns P, Van der Linden V, et al (2013) Composition data of a large collection of black-
716 appearing Roman glass. Open J Archaeom 1:22. doi: 10.4081/arc.2013.e22

717 Calas G, Cormier L, Galoisy L, Jollivet P (2002) Structure–property relationships in multicomponent
718 oxide glasses. Comptes Rendus Chim 5:831–843. doi: https://doi.org/10.1016/S1631-
719 0748(02)01459-5

720 Capobianco N, Hunault MOJY, Balcon-Berry S, et al (2019) The Grande Rose of the Reims Cathedral: an
721 eight-century perspective on the colour management of medieval stained glass. Sci Rep 9:3287.

722 doi: 10.1038/s41598-019-39740-y

723 Ceglia A, Cosyns P, Nys K, et al (2016) Light through glass: The spectrum of Late Antique glass from
724 Cyprus. J Archaeol Sci Reports 7:614–624. doi: 10.1016/j.jasrep.2015.09.024

725 Ceglia A, Cosyns P, Nys K, et al (2015a) Late antique glass distribution and consumption in Cyprus: a
726 chemical study. J Archaeol Sci 61:213–222. doi: 10.1016/j.jas.2015.06.009

727 Ceglia A, Nuyts G, Cagno S, et al (2014) A XANES study of chromophores: the case of black glass. Anal
728 Methods 6:2662–2671. doi: 10.1039/c3ay42029a

729 Ceglia A, Nuyts G, Meulebroeck W, et al (2015b) Iron speciation in soda-lime-silica glass: a comparison
730 of XANES and UV-vis-NIR spectroscopy. J Anal At Spectrom 30:1552–1561. doi:
731 10.1039/c5ja00046g

732 Chopinet M-H, Lizarazu D, Rocanière C (2002) L'importance des phénomènes d'oxydo-réduction dans
733 le verre. Comptes Rendus Chim 5:939–949. doi: 10.1016/S1631-0748(02)01455-8

734 Cicconi MR, Neuville DR, Tannou I, et al (2015) Competition between two redox states in silicate melts:
735 An in-situ experiment at the Fe K-edge and Eu L3-edge. Am Mineral 100:1013–1016. doi:
736 10.2138/am-2015-5172

737 Colorizer (2018) http://colorizer.org/

738 Cosyns P (2011) The production, distribution and consumption of black glass in the Roman Empire
739 during the 1st-5th century AD: An archaeological, archaeometric and historical approach. Vrije
740 Universiteit Brussel

741 Cosyns P, Cagno S, Janssens K, Nys K (2014) Un verre méditerranéen pour la production de bracelets
742 laténiens en Europe septentrionale. Bull l'Association française pour l'archéologie du verre 13–
743 19

744 De Ferri L, Arletti R, Ponterini G, Quartieri S (2011) XANES, UV-VIS and luminescence spectroscopic
745 study of chromophores in ancient HIMT glass. Eur J Mineral 23:969–980. doi: 10.1127/0935-
746 1221/2011/0023-2125

747 Donald SB, Swink AM, Schreiber HD (2006) High-iron ferric glass. J Non Cryst Solids 352:539–543. doi:
748 10.1016/j.jnoncrysol.2005.11.042

749 Fogolari G, Scarfì BM (1970) Adria antica. Alfieri, Edizioni d'Arte, Venezia

750 Fontaine SD, Foy D (2007) L'épave Ouest-Embiez 1, Var : le commerce maritime du verre brut et
751 manufacturé en Méditerranée occidentale dans l'Antiquité. Rev archéologique Narbonnaise
752 40:235–265. doi: 10.3406/ran.2007.1182

753 Foster HE, Jackson CM (2010) The composition of late Romano-British colourless vessel glass: glass
754 production and consumption. J Archaeol Sci 37:3068–3080. doi: 10.1016/j.jas.2010.07.007

755 Foy D (2000) Technologie, géographie, économie: les ateliers de verriers primaires et secondaires en
756 Occident. Esquisse d'une évolution de l'Antiquité au Moyen Âge. Trav la maison l'Orient
757 méditerranéen 33:147–170

758 Freestone IC (2015) The recycling and reuse of Roman glass: Analytical approaches. J Glass Stud 78:1–
759 12

760 Freestone IC (1994) Chemical analysis of "raw" glass fragments. In: Hurst HR (ed) Excavations at
761 Carthage II, 1. The Circular Harbour, North Side. Oxford University Press for British Academy,
762 Oxford, p 290

763 Freestone IC, Degryse P, Lankton J, et al (2018) HIMT, glass composition and commodity branding in
764 the primary glass industry. In: Rosenow D, Phelps M, Meek A, Freestone IC (eds) Things that
765 Travelled: Mediterranean Glass in the First Millennium AD. UCL Press, London (UK), pp 159–190

766 Freestone IC, Stapleton CP (2015) Composition of mosaic glass vessels of the early Imperial period. In:
767 Bayley J, Freestone I, Jackson C (eds) Glass of the Roman world. Oxbow Books, pp 61–76

768 Gallo F, Silvestri A, Molin G (2013) Glass from the Archaeological Museum of Adria (North-East Italy):
769 new insights into Early Roman production technologies. J Archaeol Sci 40:2589–2605. doi:
770 10.1016/j.jas.2013.01.017

771 Ganio M, Boyen S, Fenn T, et al (2012) Roman glass across the Empire: an elemental and isotopic
772 characterization. J Anal At Spectrom 27:743–753. doi: 10.1039/c2ja10355a

773 Gliozzo E (2017) The composition of colourless glass: a review. Archaeol Anthropol Sci 9:455–483. doi:
774 10.1007/s12520-016-0388-y

775 Gliozzo E, Santagostino Barbone A, D'Acapito F, et al (2010) The Sectilia Panels of Faragola (Ascoli
776 Satriano, Southern Italy): a Multi-Analytical Study of the Green, Marbled (Green and Yellow), Blue
777 and Blackish Glass Slabs. Archaeometry 52:389–415. doi: 10.1111/j.1475-4754.2009.00493.x

778 Gliozzo E, Turchiano M, Giannetti F, Santagostino Barbone A (2016) Late Antique glass vessels and
779 production indicators from the town of Herdonia (Foggia, Italy): New data on CaO-rich/weak
780 HIMT glass. Archaeometry 58:81–112. doi: 10.1111/arcm.12219

781 Hunault MOJY, Bauchau F, Loisel C, et al (2016) Spectroscopic Investigation of the Coloration and
782 Fabrication Conditions of Medieval Blue Glasses. J Am Ceram Soc 99:89–97. doi:
783 10.1111/jace.13783

784 Hunault MOJY, Loisel C, Bauchau F, et al (2017) Nondestructive Redox Quantification Reveals
785 Glassmaking of Rare French Gothic Stained Glasses. Anal Chem 89:6277–6284. doi:
786 10.1021/acs.analchem.7b01452

787 Iyel A, Oktem D, Akmaz F (2014) Parameters affecting the color mechanism of manganese containing
788 colored glasses. J Chem Chem Eng 9:849–858. doi: 10.17265/1934-7375/2014.09.002

789 Jackson CM (2005) Making colourless glass in the Roman period. Archaeometry 47:763–780. doi:
790 10.1111/j.1475-4754.2005.00231.x

791 Jackson CM, Paynter S (2015) A Great Big Melting Pot: Exploring Patterns of Glass Supply, Consumption
792 and Recycling in Roman Coppergate, York. Archaeometry 58:68–95. doi: 10.1111/arcm.12158

793 Janssens K (2013) Modern Methods for Analysing Archaeological and Historical Glass. John Wiley &
794 Sons, Ltd, Chichester, West Sussex, United Kingdom

795 Johnston-Feller R (2001) Color science in the examination of museum objects. Nondestructive
796 procedures. The Getty Conservation Institute, Los Angeles

797 Kido L, Müller M, Rüssel C (2005) High temperature spectroscopy of manganese and chromium doped
798 glasses with the basic composition 16Na2O • 10CaO • 74SiO2. J Non Cryst Solids 351:523–529.
799 doi: 10.1016/j.jnoncrysol.2005.01.033

800 Kress VC, Carmichael ISE (1988) Stoichiometry of the iron oxidation reaction in silicate melts. Am
801 Mineral 73:1267–1274. doi: 0003-004x/88 / rrr2-r267s02.00

802 Maltoni S, Silvestri A (2018) A mosaic of colors: Investigating production technologies of Roman glass
803 tesserae from Northeastern Italy. Minerals 8:255. doi: 10.3390/min8060255

804 Maltoni S, Silvestri A, Marcante A, Molin G (2016) The transition from Roman to Late Antique glass:
805 new insights from the Domus of Tito Macro in Aquileia (Italy). J Archaeol Sci 73:1–16. doi:
806 10.1016/j.jas.2016.07.002

807 Marcus RT (1998) The measurement of color. In: Nassau K (ed) Color for Science, Art and Technology.
808 Elsevier, pp 31–96

809 Mendera M, Cantini F, Marcante A, et al (2017) Where does the medieval glass from San Genesio (Pisa,
810 Italy) come from? In: Wolf S, de Pury-Gysel A (eds) Annales du 20e Congrès de l'Association
811 Internationale pour l'Histoire du Verre, Fribourg – Romont (Suisse). Verlag Marie Leidorf GmbH,
812 pp 360–366

813 Meulebroeck W, Baert K, Wouters H, et al (2010) The identification of chromophores in ancient glass
814 by the use of UV-VIS-NIR spectroscopy. In: Proc. SPIE 7726 Optical Sensing and Detection. pp

77260D, 12 pages

Mirti P, Pace M, Negro Ponzi MM, Aceto M (2008) ICP–MS Analysis of Glass Fragments of Parthian and Sasanian Epoch From Seleucia and Veh Ardašīr (Central Iraq). Archaeometry 50:429–450. doi: 10.1111/j.1475-4754.2007.00344.x

Mokrzycki W, Tatol M (2011) Color difference ΔE - A survey. Mach Graph Vis 20:383–411

Möncke D, Papageorgiou M, Winterstein-Beckmann A, Zacharias N (2014) Roman glasses coloured by dissolved transition metal ions: redox-reactions, optical spectroscopy and ligand field theory. J Archaeol Sci 46:23–36. doi: 10.1016/j.jas.2014.03.007

Müller-Simon H (2011) Fining of glass melts. Rev Mineral Geochemistry 73:337–361. doi: 10.2138/rmg.2011.73.12

Newton R, Davison S (1996) Conservation of Glass. Butterworth Heineman, Oxford, UK

Paul A (1982) Chemistry of glasses. Chapman and Hal, London (UK), New York (USA)

Paynter S (2006) Analyses of colourless Roman glass from Binchester, County Durham. J Archaeol Sci 33:1037–1057. doi: 10.1016/j.jas.2005.10.024

Paynter S, Jackson CM (2016) Re-used Roman rubbish: a thousand years of recycling glass. Eur J Post Class Archaeol 6:31–52. doi: 10.1002/eji.201242477

Quartieri S, Arletti R (2013) The Use of X-Ray Absorption Spectroscopy in Historical Glass Research. In: Janssens K (ed) Modern Methods for Analysing Archaeological and Historical Glass. John Wiley & Sons, Ltd., Chichester, West Sussex, United Kingdom, pp 301–309

Quartieri S, Riccardi MP, Messiga B, Boscherini F (2005) The ancient glass production of the Medieval Val Gargassa glasshouse: Fe and Mn XANES study. J Non Cryst Solids 351:3013–3022. doi: 10.1016/j.jnoncrysol.2005.06.046

Rehren T, Connolly P, Schibille N, Schwarzer H (2015) Changes in glass consumption in Pergamon (Turkey) from Hellenistic to late Byzantine and Islamic times. J Archaeol Sci 55:266–279. doi: 10.1016/j.jas.2014.12.025

Rosenow D, Rehren T (2014) Herding cats – Roman to Late Antique glass groups from Bubastis, northern Egypt. J Archaeol Sci 49:170–184. doi: 10.1016/j.jas.2014.04.025

Rüssel C (1989) Redox reactions during cooling of glass melts - A theoretical consideration. Glas Berichte Zeitschr für Glas 62:199–203

Rüssel C (2005) Redox behavior and electrochemical behavior of glass melts. In: Pye D, Joseph I,

845 Montenero A (eds) Properties of Glass-Forming Melts. CRC Press, pp 27–55

846 Sayre E V. (1963) The intentional use of antimony and manganese in ancient glasses. In: Matson FR,
847 Rindone GE (eds) Advances in glass technology: history papers and discussions of the technical
848 papers of the VI International Congress on Glass. Plenum Press, New York, pp 236–282

849 Schibille N, Meek A, Tobias B, et al (2016) Comprehensive chemical characterisation of Byzantine glass
850 weights. PLoS One 11:1–26. doi: 10.1371/journal.pone.0168289

851 Schibille N, Sterrett-Krause A, Freestone IC (2017) Glass groups, glass supply and recycling in late
852 Roman Carthage. Archaeol Anthropol Sci 9:1223–1241. doi: 10.1007/s12520-016-0316-1

853 Schreiber HD (1987) An electrochemical series of redox couples in silicate melts: a review and
854 applications to geochemistry. J Geophys Res - Solid Earth 92:9225–9232. doi:
855 https://doi.org/10.1029/JB092iB09p09225

856 Schreiber HD (1986) Redox processes in glass-forming melts. J Non Cryst Solids 84:129–141. doi:
857 10.1016/0022-3093(86)90770-2

858 Schreiber HD, Balazs BG, Carpenter BE, et al (1984) An electromotive force series in a borosilicate glass-
859 forming melt. J Am Ceram Soc 67:C106–C108. doi: 10.1111/j.1151-2916.1984.tb19710.x

860 Schreiber HD, Merkel RCJ, Schreiber L V., Balazs BG (1987) Mutual interactions of redox couples via
861 electron exchange in silicate melts - Models for geochemical melt systems. J Geophys Res - Solid
862 Earth 92:9233–9245. doi: 10.1029/JB092iB09p09233

863 Schreiber HD, Peters LJ, Beckman JW, Schreiber CW (1996) Redox chemistry of iron-manganese and
864 iron-chromium interactions in soda lime silicate glass melts. Glas Sci Technol 69:269–277

865 Schreiber HD, Wilk NR, Schreiber CW (1999) Comprehensive electromotive force series of redox
866 couples in soda-lime-silicate glass. J Non Cryst Solids 253:68–75. doi: 10.1016/S0022-
867 3093(99)00344-0

868 Schreiber HD, Wood JG, Schreiber CW (2000) Effectiveness of oxidizing agents on the iron redox state
869 in glasses. Glas Sci Technol BERICHTE 73:213–222

870 Sharma G, Bala R (2003) Digital color imaging handbook, 1st Editio. CRC Press

871 Shelby JE (2005) Introduction to Glass Science and Technology, Edition 2. Royal Society of Chemistry,
872 Cambridge

873 Silvestri A (2008) The coloured glass of Iulia Felix. J Archaeol Sci 35:1489–1501. doi:
874 10.1016/j.jas.2007.10.014

875 Silvestri A, Gallo F, Maltoni S, et al (2018) Things that travelled - A review of the Roman glass from
876 Northern Adriatic Italy. In: Daniela Rosenow D, Phelps M, Meek A, Freestone IC (eds) Things That
877 Travelled: Mediterranean Glass in the First Millennium CE. UCL Press, London (UK), pp 346–367

878 Silvestri A, Molin G, Salviulo G (2008) The colourless glass of Iulia Felix. J Archaeol Sci 35:331–341. doi:
879 10.1016/j.jas.2007.03.010

880 Silvestri A, Molin G, Salviulo G (2005) Roman and Medieval glass from the Italian area: Bulk
881 characterization and relationships with production technologies. Archaeometry 47:797–816. doi:
882 10.1111/j.1475-4754.2005.00233.x

883 Silvestri A, Tonietto S, Molin G (2011) The palaeo-Christian glass mosaic of St. Prosdocimus (Padova,
884 Italy): archaeometric characterisation of 'gold' tesserae. J Archaeol Sci 38:3402–3414. doi:
885 10.1016/j.jas.2011.07.027

886 Silvestri A, Tonietto S, Molin G, Guerriero P (2014) The palaeo-Christian glass mosaic of St. Prosdocimus
887 (Padova, Italy): Archaeometric characterisation of tesserae with copper- or tin-based opacifiers.
888 J Archaeol Sci 42:51–67. doi: 10.1016/j.jas.2013.10.018

889 Silvestri A, Tonietto S, Molin G, Guerriero P (2012) The palaeo-Christian glass mosaic of St. Prosdocimus
890 (Padova, Italy): archaeometric characterisation of tesserae with antimony- or phosphorus-based
891 opacifiers. J Archaeol Sci 39:2177–2190. doi: 10.1016/j.jas.2012.03.012

892 Silvestri A, Tonietto S, Molin G, Guerriero P (2015) Multi-methodological study of palaeo-Christian glass
893 mosaic tesserae of St. Maria Mater Domini (Vicenza, Italy). Eur J Mineral 27:225–245. doi:
894 10.1127/ejm/2015/0027-2427

895 Simpson W, Myers DD (1978) The redox number concept and its use by the glass technologist. Glas
896 Technol 19:82–85

897 Toniolo A (2007) "...pallentia solphurata fractis permutat vitreis...". Il carico di rottami del relitto di
898 Grado. In: XI Giornate Nazionali di Studio, Il Vetro dell'Alto Adriatico. Ferrara, pp 57–69

899 Van Der Linden V, Cosyns P, Schalm O, et al (2009) Deeply Coloured and black glass in the northern
900 provinces of the Roman empire: differences and similarities in chemical composition before and
901 after AD 150. Archaeometry 51:822–844. doi: 10.1111/j.1475-4754.2008.00434.x

902 Vanhoutte S (2007) Het Romeinse castellum van Oudenburg (prov. West-Vlaanderen) herontdekt: de
903 archeologische campagne van augustus 2001 tot april 2005 ter hoogte van de zuidwesthoek.
904 Interim-rapport. Relicta 3:199–236

905 Vercamer V, Lelong G, Hijiya H, et al (2015) Diluted Fe3+ in silicate glasses: Structural effects of Fe-

redox state and matrix composition. An optical absorption and X-band/Q-band EPR study. J Non Cryst Solids 428:138–145. doi: https://doi.org/10.1016/j.jnoncrysol.2015.08.010

Weyl WA (1951) Coloured glasses, Society of. The Society of Glass Technology

Whitehouse D (2004) Glass in the price edict of Diocletian. J Glass Stud 46:189–191

Zoleo A, Brustolon M, Barbon A, et al (2015) Fe(III) and Mn(II) EPR quantitation in glass fragments from the palaeo-Christian mosaic of St. Prosdocimus (Padova, NE Italy): Archaeometric and colour correlations. J Cult Herit 16:322–328. doi: 10.1016/j.culher.2014.07.005